International Journal of Engineering Research & Technology (IJERT)
ISSN: 2278-0181
Vol. 7 Issue 05, May-2018

Laser Parameters Effect on the Structure and Properties of Nickel

Danavath. Balu
Assistant Professor
Department of Mechanical Engineering
Sri Indu College of Engineering and Technology
UGC Autonomous Institution, Recognized under 2(f) and 12(B) of UGC Act 1956
Sheriguda , Ranga Reddy (Dist)-510501, Telangana, India

Abstract **This project deals with the study of effect of LASER power and LASER beam scan speed"over the morphological and structural changes in Nickel material and correlating this with the mechanical properties. Surface modification has been done by Diode laser for uniform penetration depth. Several experiments have been carried out on Nickel in the presence Inert gas (Argon) by varying parameters (LASER power, scan speed). Powder x-ray diffraction, optical microscopy and scanning electron microscopy techniques were used to observe the morphological and structural changes. Vickers's hardness test was used to measure the hardness of modified surface. Formation of new phase was confirmed from the imaging (microscopy), diffraction (XRD) analysis. An increment in the hardness of material was observed which is in agreement with the formation of new phase.**

Key points: Laser-Matter Interaction; Laser Parameters; Structure-Property correlation.

Table 1. Chemical composition of Nickel

Physical constants	Density (gm./cc)	Melting Range (ºC)	Specific Heat (J/Kg.ºC)	Curie Temperature (ºC)
Values	8.89	1435-1446	456	360

1. INTRODUCTION

1.1. Metallographic

Nickel is a solid-solution alloy with a face-centered cubic structure. Nickel is 99.0% pure wrought nickel. It is known for its superior mechanical properties and resistance to corrosive environments. Some other useful properties of the alloy are its magnetic and magnetostrictive properties. Nickel has high thermal and electrical conductivities. Table 1 [1] shows the chemical composition of Nickel . The anti-corrosive nature of Nickel finds its use in chemical shipping drums, missile components, food handling drums and for other structural applications where corrosion resistance is given prime consideration [1].

1.2. Physical properties of Nickel

Physical constants and thermal properties are shown in Table 2. [1]

Table 2. Physical properties

Elements		Nickel	Copper	Iron	Manganese	Carbon	Silicon
Chemical Composition (%)	99.0	0.25	0.4	0.35	0.15	0.35	

1.3. Mechanical Properties

Mechanical properties of Nickel are shown in Table 3. [1]

Table 3. Mechanical properties of nickel

Mechanical properties	Values
Tensile Strength (MPa)	585
Yield Strength (MPa)	310
Young's Modulus (GPa)	205
Shear Modulus (GPa)	79.6
Poisson'sRatio	0.29
Elongation (%)	55
Rockwell Hardness B	80

1.4. Corrosion resistance

It has good resistance to normal and many other corrosive media. It can be used in both reducing and oxidizing environments. The resistance of Nickel to caustics is due to the development of a passive film of its oxide [1].

1.5. High-temperature properties

Service temperatures of pure Nickel are usually limited below 315°C because at components under ASME Boiler and Pressure Vessel standards [1].

International Journal of Engineering Research & Technology (IJERT)
ISSN: 2278-0181
Vol. 7 Issue 05, May-2018

1.2 Laser

1.2.1. Laser generation

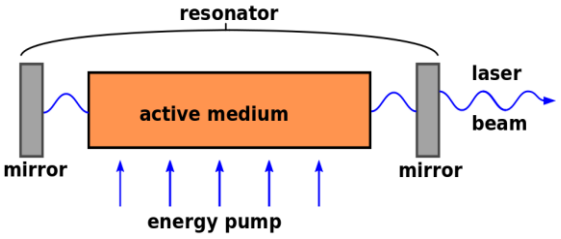

Fig-1: Basic schematic of a laser

The laser system essentially has a gain medium, placed between pair parallel mirrors. One of them partially transmitting and another mirror is highly reflecting. An energy source is pump to active medium. The gain media may be gas, solid or liquid and the gain media have the property to magnify the amplitude of the light wave passing through gain media by stimulated emission. The gain media place in between the two mirrors such that light oscillating between two mirrors passes all time through the gain medium.

1.2.2. Laser physics

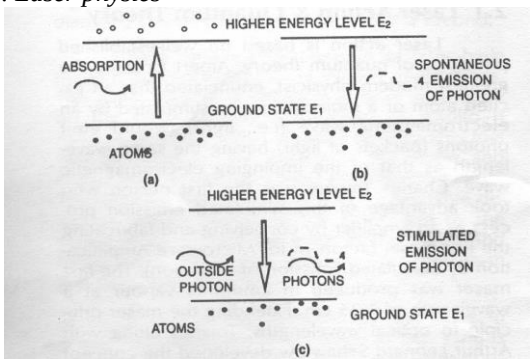

Fig-2: Laser principle

1.2.3. Laser energy absorption

The one of the most important feature of laser light is ability to transfer very high values of irradiance of selected surface of the material this can generate the very rapid heating on the small area of material. This very rapid localized heating leads to many applications in the material processing.The absorption of laser energy is by materials, it includes the losses of energy from that result from reflection.

When light strikes an opaque surface, it is absorbed within a thin layer located near the surface. The absorbed according to the equation

$$I(x) = I_0 \exp(-ax)$$

Where, I_o = is the incident intensity

$I(x)$ = the intensity reaching from depth x from the surface

a = absorption coefficient, with units of reciprocal centimeters.

The light (at least 63% of it) is absorbed within a depth of 1/a from the surface. Then can be transported to depth by thermal conduction

1.2.4. Laser parameters

Laser can be characterized Physical parameters such as temporal and spatial properties of output light, resonator design and active element producing the light and pumping method. Laser parameters describe the physical state of the light which is coming from laser. The one of the most important characteristics for material processing is spatial coherence. The very important in the material processing is spatial properties of laser light such as ability to focus on small area (spot).Laser can be operated in different temporal mode (i.e. either continuous or pulses the time ranges from milliseconds to femtoseconds. In the material processing the continuous wave laser is used. Table 5 describes the laser parameters.

Table 4: laser parameters.

Laser parameters	Symbols/equation
Laser beam power	P
Laser beam width	D
Laser beam energy	E
Wavelength	λ
Full width diffraction angle	$\theta_{diff}= 2\lambda/D$
Focal spot diameter	$D_{foc} =2\lambda f/DE$
Laser beam scan speed	mm/sec

2. EXPERIMENTAL PROCEDURE

2.1 Sample Preparation

The pure Nickel (200) was used to carry out the heat treatment and laser treatment experiment. The samples were cut from the main block into small specimen pieces. The original dimensions of the as received sample are 15mm in length, 15mm in width and 3mm in thickness as shown in the figure 3.

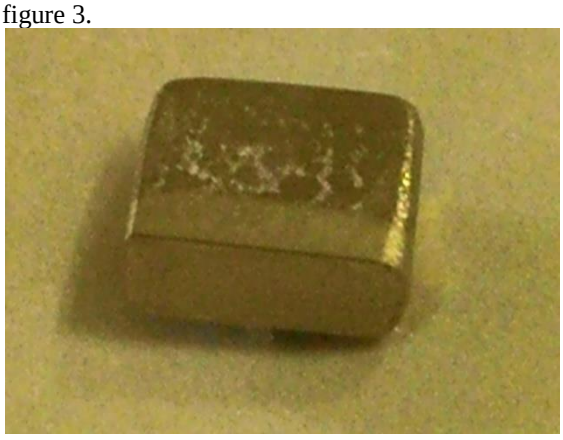

Fig-3: As received Sample Nickel

International Journal of Engineering Research & Technology (IJERT)
ISSN: 2278-0181
Vol. 7 Issue 05, May-2018

2.2. Laser Instrument

The laser treatment carried out on as received sample pure Nickel (200), the name of the laser instrument is Fiber coupled diode laser, which is having Continuous wave laser and with 200 to 6 kW power with wave length 915, 940 and 980 nm was use. Circular spot with 1.5 and 3 mm diameter and rectangular spot with 4x4, 5x20, 1.5x11, 2x17 and 5x8 mm^2.Laser optic head is fixed of 6-axis Robot arm and two additional rotary and tilt axis integrated with system. Reach of 2.3 m is possible. Temperature up to 1400^oC at 50 Hz measuring rate can be measured by lateral-resolving system (E-MAQS). And attached with pyrometer and can measure up to 2500^oC.

Fig- 4: Fiber coupled diode laser

2.3. Laser Treatment Experimental Procedure

Table 5. Laser parameters used in experiment.

Laser power(W)	Laser Scanning Speed (mm/second)	Laser beam size (mm^2)	Wave length (nm)	Argon gas Pressure (bar)
2500	15	5x8	980	1

2.4. Sample characterization Techniques

The topography and structure of the as-prepared, heat treatment and laser treated sample of nickel were characterized by visible light optical microscopy(OPM, OLYMPUS), scanning electron microscopy (SEM, HITACHI S-3400 N), Energy Dispersive X-ray spectroscopy (EDS), and Powder X-ray diffraction (XRD, Bruker, D8 Advance) and Vickers's hardness testing (UHL,VMHT DIN 50 133).

3. RESULTS AND DISCUSSION

3.1. Optical microscopy analysis

The microstructure studies of as received, heat treated and laser treated samples has been carried out using visible light microscopy. Figure 6 shows the optical micrographs of as received and heat treated sample, the micrographs taken at 100X magnification.

3.2. Cross-sectional view of Nickel

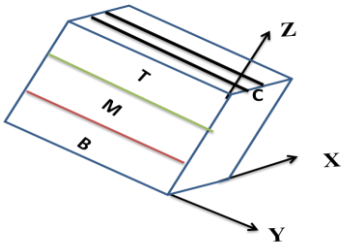

Fig-5:Cross-sectional view of Nickel

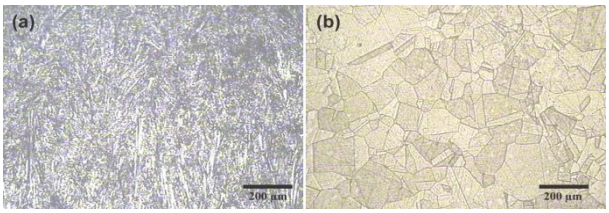

Fig-6: The cross-sectional view optical micrographs of (a) as received sample, (b) heat treated sample respectively. Magnification is 100X.

3.3 .Optical Micrographs of Laser treated Samples

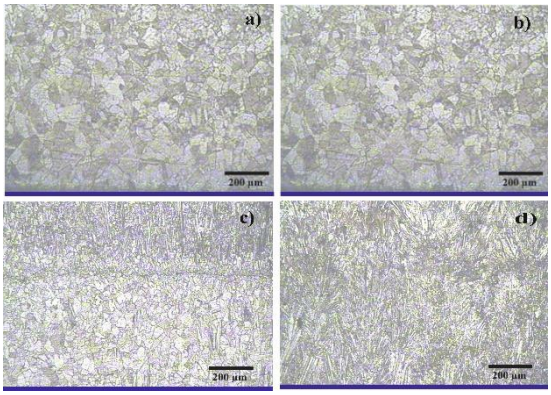

Fig-7: The cross-sectional view optical micrographs of laser treated sample-1, (a) to (d) indicates from top to bottom regions at 100X magnification

Figure 7 shows the micrographs of the sample-1, (Fig 7(a) to fig 7(d)) shows top region to bottom region. The laser power and laser beam scan speed were shown on the top of micrographs. The laser scan speed was faster but, power was high so, the recovery, recrystallization and grain growth are taken place, whereas at middle region only recovery and recrystallization were taken place. Therefore the coarse grains were observed at top region and finer grains were observed at middle region. The more heat generation at the top region than other regions. The bottom region was appearing as cast structure as that of as received region (Fig 7(a)). The grain size was decreased from top region to interface region.

International Journal of Engineering Research & Technology (IJERT)
ISSN: 2278-0181
Vol. 7 Issue 05, May-2018

3.4. Scanning Electron Microscopy
3.4.1.Sample-1 2500W for 15mm/s)

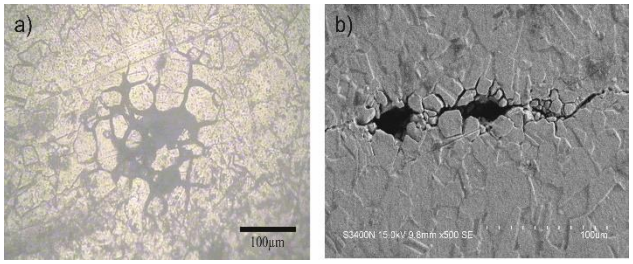

Fig-8: The cross-sectional view of (a) Optical micrographs of cracked region of sample-1, (b)Scanning electron micrograph of cracked region of sample-1,

Figure 8 shows the scanning electron micrographs of sample-1 that are taken at 500X magnification. Micro cracks have been observed in between the top region and the middle region. In this region rapid expansion and rapid contraction are taken place, due to this rapid cooling cracks were formed at the interface region. Micro cracks have been observed in the entire laser treated samples. These micro cracks were propagating along the grain boundary of the samples is called as Intergranular crack.Intergranular fracture is the propagation of cracks along the grain boundaries of a metal or alloy. It is a fracture that follows the grain boundaries of the material.This usually occurs when the phase in the grain boundary is weak and brittle. Intergranular cracking is not visible on the surface and is very destructive.

3.5. Energy Dispersive Spectroscopy (EDS) of laser treated sample

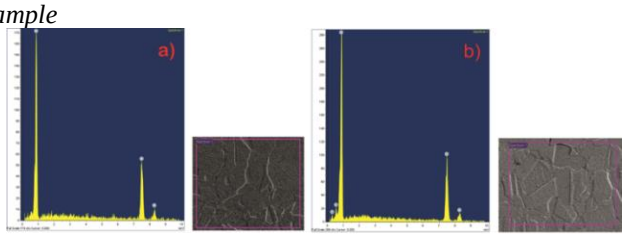

Elements	weight(%)	Atomic(%)
Ni L	100.0	100.0
Total	100.0	

Elements	weight(%)	Atomic(%)
C K	3.45	20.06
O K	2.21	6.37
Ni L	92.34	72.67
Total	100.0	

Fig-9: cross-sectional view of Energy Dispersive Spectroscopy (EDS) of laser treated sample. (a) Energy Dispersive Spectroscopy (EDS) of sample-1.

For chemical composition analysis the Energy Dispersive Spectroscopy (EDS) was carried out for all laser treated samples. Figure 9 shows the sample -1 of chemical composition is 100 % pure Nickel,

3.6. X-ray diffraction analysis of as received and Heat Treated Samples

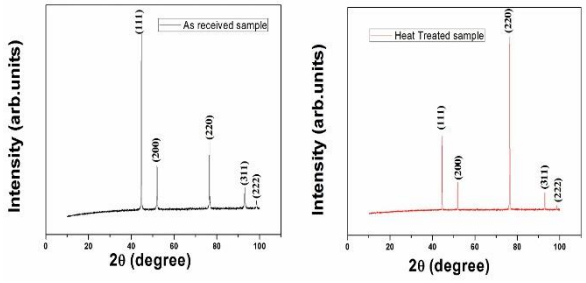

Fig-10: X-ray diffraction (XRD) patterns of nickel in as received and heat treated samples

Figure.10 shows the X-ray Diffraction (XRD) patterns of nickel in as received and heat treated conditions. The crystal structure is determined as face centered cubic and all the peaks are indexed according to that. By comparing both the XRD patterns, it was confirmed that there was no phase change occurred during the heat treatment. The (111) peak intensities was high in as received sample because of more number of grains were oriented in this plane. Whereas in the heat treated sample after heat treatment, the (220) peak intensity was higher because of more number of grains were oriented in this plane, moreover peaks becomes sharper in heat treated samples.

3.7. X-ray diffraction analysis Laser Treated Samples

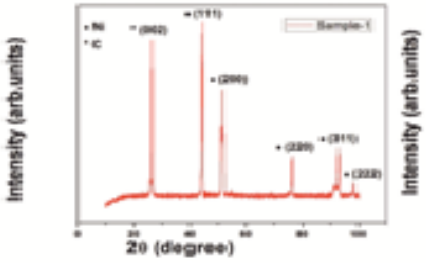

Fig-11: X-ray diffraction (XRD) patterns of laser treated samples-1

Figure11 shows the XRD patterns of laser treated samples with different laser parametrs.In comparison of peak positions of laser treated samples with that of as received samples, it is evident that, there was no NiO was presented in sample-1. But, in this sample scan speed was faster so rapid heating and rapid cooling is taken place. The splitting of peaks was observed due to a small lattice distortion in certain crystallographic directions caused by laser irradiation. This distortion due to the thermal stresses, the strain present in the sample-1 the peaks were broadening. The crystal structure of sample is determined as face centered cubic. All the peaks are shifts towards lefts (in comparison with as received). This is indicating the presence of tensile residual stresses in the sample

.

International Journal of Engineering Research & Technology (IJERT)
ISSN: 2278-0181
Vol. 7 Issue 05, May-2018

3.8. Vickers's hardness test

Table.6 vicker's hardness test

Samples	HV	MPa
As received sample	169.8	1666
Heat treated sample	94.5	927.69

Vickers hardness testing carried out on the cross-section of the as received sample; heat treatment sample and different laser treated samples were performed. The three regions such as top region, middle region, and bottom region were selected forthe hardness tests on the cross-section of samples at 50 gf loads. Table 12 Shows the Vickers hardness values of received and heat treated sample.

Table 7. Vickers's hardness test for as received sample and heat treatment sample.

Sample Surface	HV	MPa
Top Surface	151.3	1484
Middle Surface	163.6	1605
Bottom Surface	158.3	1553

Table 7 shows the variation of Vickers hardness with the thickness of the laser treated samples. In the smallest grain size range, the Vickers hardness is increases with decreasing grain size. This so called reverse Hall-Petch, and this behavior has been observed in Vickers hardness test of the laser treated samples-1. Vickers hardness is less, in the middle region the grain size is less, the Vickers hardness is gradually increases and in the bottom region the grain size is more as a result the Vickers hardness is less.

4. CONCLUSIONS

- Optical microscopy revealed large grain size analysis, of laser treated samples there is maximum grain size at top region, minimum grain size at middle region and maximum grains at bottom regions. This trend was observed in all laser treated samples.
- At laser scanning speed of 15mm/sec, the microstructure shows as cast dendritic structure near the bottom of the sample-1 and lattice distortion was observed from XRD studies.
- From the scanning electron microscope, at interface region the intergranular cracks (micro cracks) were observed in all laser treated samples.
- From the Vickers hardness testing, hardness was minimum at top region, maximum at middle region and minimum at bottom region. This trend was observed in all the laser treated samples.

REFERENCES

[1] Special Metals Corporation. "Publication Number SMC-061: Nickel 200 & 201," pp.1–19, 2006.
[2] B. S. Yilbas, S. Akhtar, and C. Karatas, "Laser surface treatment of pre-prepared Rene 41 surface," Opt. Lasers Eng., vol. 50, no. 11, pp. 1533–1537, 2012.
[3] J. A. Bailey, ASM Handbook, ASM International Materials Selection and Design, Volume 8 (2000), 416-470
[4] M. Metallurgy, P. Table, M. Bonding, I. Bonding, C. Bonding, S. Bonding, S. Lattices, and C. Systems, "© 2008 ASM International. All Rights Reserved. Elements of Metallurgy andEngineeringAlloys(#05224G) www.asminternational.org," 2008.
[5] M. S. Brown and C. B. Arnold, "Laser PrecisionMicrofabrication,"Springer Ser. Mater. Sci., vol. 135, no. 0933–033X, pp. 91–120, 2010.
[6] T. L. Lin and D. McLean, "Changes Produced by Deformation in Grains and Grain Boundaries of Nickel," Met. Sci., vol. 2, no. 1, pp. 108–113, 1968.
[7] I. Dlouhy, M. Tarafder, and H. Hadraba, "Micromechanical Aspects of Transgranular and Intergranular Failure Competition," Key Eng. Mater., vol. 465, pp. 399–402, 2011.
[8] R. Cottam, "Laser Materials Processing for Improved Corrosion Performance," pp. 3–18, 2012.
[9] X. Ye, J. Long, Z. Lin, H. Zhang, H. Zhu, and M. Zhong, "Direct laser fabrication of large-area and patterned graphene at room temperature," Carbon N. Y., vol. 68, pp. 784–790, 2014.
[10] Metallography: Principles and practice, vol. 18, no. 3. 1985.
[11] G.Phanikumar, P.Dutta, and K. Chattopadhyay, "Continuous welding of Cu–Nidissimilar couple using CO₂ laser," Sci. Technol. Weld. Join., vol. 10, no. 2, pp. 158–166, 2005